

The Corrosion Resistance of Trivalent Chrome Conversion Coatings on Zinc Electroplated Steel in Accelerated Test Conditions and After Natural Exposure

Nguyen Thi Thanh Huong, Le Ba Thang, Le Duc Bao, Nguyen Van Khuong and Dao Bich Thuy
Institute for Tropical Technology, Vietnam Academy of Science and Technology, 18 Hoang Quoc Viet, Cau Giay, Ha Noi.

ARTICLE INFO

Article history:

Received: 29 July 2019;

Received in revised form:

27 August 2019;

Accepted: 7 September 2019;

Keywords

Trivalent Chrome Conversion Coatings,
Zinc Electroplated Steel,
Salt Spray Test,
Atmospheric Corrosion,
SEM,
Corrosion Products.

ABSTRACT

The corrosion resistance of trivalent chrome conversion coatings on electroplated zinc is studied and compared with that of hexavalent chrome conversion coatings in salt spray testing conditions. The trivalent chrome conversion coatings and hexavalent chrome conversion coatings were unstable at pH 3. All samples had more than 5 % of the surface area covered with white rust after 24 hours of salt fog exposure. The corrosion resistance of the samples is as follows: TM 3108 ~ SP 25 > 747 at pH 6.5. The highest resistance obtained on the TM 3108 with white rust appeared after 400 hours of salt fog exposure. All of the hexavalent chrome conversion coatings and trivalent chrome conversion coatings had corrosion current densities ($1.26 \times 10^{-7} \div 1.82 \times 10^{-7}$ A/cm²) much smaller than corrosion current density of the zinc electrodeposited sample (7.7×10^{-6} A/cm²). The compositions of corrosion products of the sample surfaces after exposure were investigated. The results of analysis by means of X-ray diffraction showed that the corrosion products formed on zinc coatings, trivalent and hexavalent CCCs in atmospheric conditions of Hanoi had the distinctions specialty of the humid tropical climates. Zinc sulfate hydroxide hydrate $Zn_4SO_4(OH)_6 \cdot H_2O$; Zinc carbonate hydroxide hydrate $Zn_4CO_3(OH)_6 \cdot H_2O$; Simonkolleite $Zn_5(OH)_8Cl_2 \cdot H_2O$; Chromium Sulfate $Cr_2(SO_4)_3$; Zinc chloride sulfate hydroxide hydrate $Zn_{12}(OH)_{15}(SO_4)_3Cl_3 \cdot H_2O$; Eskolaite Cr_2O_3 had been identified. The presence of SO_2 resulted in the formation of Zinc sulfate hydroxide hydrate $Zn_4SO_4(OH)_6 \cdot H_2O$. After 5 years of exposure in atmospheric conditions, the hexavalent CCCs on zinc coatings had show the best corrosion resistance and the least corrosion products. The corrosion resistance of the samples decreased in the order: 747 > SP25 ~ TM 3108 > Zn.

© 2019 Elixir All rights reserved.

1. Introduction

Zinc coating is widely used to protect carbon steels against corrosion since it behaves as a barrier layer to inhibit the carbon steel from oxidation by outdoor exposure. Zinc coating also provides galvanic protection, as a sacrificial anode, for exposed areas of the steel substrates [1,2]. The corrosion resistance of zinc coating is improved by means of chemical surface treatments and organic coatings. After the application of the zinc coating on carbon steels, the chromate conversion coatings are subsequently applied to provide colors and protection against corrosion. However, certain Cr(VI) compounds are classified as carcinogens due to the intrinsic toxicity, and government legislation has limited their usage by the RoHS directives from the European Union since 2006. Trivalent chrome conversion coatings have become promising alternatives to traditional Cr(VI), because the Cr(III) treatment solutions are less toxic than Cr(VI) compounds [3]. Trivalent chrome conversion coating is one of the most effective treatments, which provides more corrosion resistance and increases the adhesion between primer coatings and metal substrates [4-6]. The salt spray test is one of the most widely used accelerated test methods for evaluating the corrosion protection provided by coatings on

metals. The intent of the salt spray test is to compare the relative corrosion resistance of specimens or evaluate the differences between a test sample and a part that has been previously tested and shown to provide satisfactory service. The test is continuously used since this is the standard that has been accepted by the industry for severe corrosion testing and it has been used historically for this purpose.

In this paper, hexavalent chrome conversion coatings and trivalent chrome conversion coatings have been investigated using the salt spray test according to the standard JIS H8502 [7]. The aim is to compare the durability of these coatings in a salt fog. The atmospheric corrosion resistance of trivalent chrome conversion coating on zinc coating is studied and compared with hexavalent chrome conversion coating and zinc coating after 5 years natural exposure in Ha Noi.

2. Materials And Methods

SPHC steel specimens were cut into size 100 x 50 x 1.2 mm. Chemical composition of the SPHC steel sheet is in accordance with JIS G3131. The specimens were prepared by mechanically polishing with sandpaper 280, 400 and 600, degreasing, and acidic pickling.

The specimens were activated with 5 % HCl(aq) for 5s. Zinc electrodeposition procedure was carried out in a bath of

25 liters containing: ZnCl₂ 60 g/l, NH₄Cl 250 g/l, AZA 0 ml/l, AZB 1.5 ml/l, pH 4.8 – 5.4, using current density 2A/dm², time 30 minutes at room temperature: (according to the process Enthone) [8].

The coating time was 30 minutes for each specimen, average thickness of the zinc coatings was 13 μm. The zinc electroplating surface was activated with 0.5 % HNO₃(aq) for 5 seconds and then rinsed in a deionized water before the conversion treatment.

The Cr(VI) and Cr(III) treatments were carried out in three different solutions:

One bath was Udycro 747 (Enthone). The specimens were treated in the bath for 30 seconds at room temperature. After rinsing in deionized water, these coatings were dried in an oven at 50 °C for 30 minutes.

The second bath was SpectraMATE 25 (Columbia). The specimens were treated in the bath at 30 °C for 60 seconds. These coatings were rinsed in deionized water and then dried in an oven at 80 °C for 30 minutes.

The third bath was TM 3108 (this is a product of VAST research project by Institute for Tropical Technology, VAST), the specimens were treated in the bath at 30 °C for 60 seconds. These coatings were rinsed in deionized water and then dried in an oven at 80 °C for 30 minutes.

Bath pH was adjusted to different values by adding HNO₃ or NH₄OH to the bath. The specimens were kept in a decicator for 48 hours at room temperature before surface analysis and corrosion tests.

The specimens were ultrasonically cleaned in ethanol for 5 minutes. The surface morphology of treated specimens was investigated by means of SEM, HITACHI S4800. The composition of corrosion products formed on specimens was investigated using XRD. In this study, the specimens were cut into 1 cm × 2 cm for XRD and 1 cm × 1 cm for the SEM analyses.

The salt spray testing of these treated samples was performed on Q-FOG CCT-600 according to the standard JIS H8502. The samples were exposed to 5 % NaCl fog (pH changing from 3.0 to 6.5 adjusted with NaOH or CH₃COOH solution by means of METERLAB PHM210) in a salt spray chamber at 35 °C. The coverage of the sample surfaces by the white corrosion products was recorded.

The corrosion behavior of the conversion coatings was evaluated by polarization tests. Polarization tests were performed at a scan rate of 2 mV/s in 5 % NaCl solution using electrode, saturated calomel electrode (SCE) as a reference a

conventional three-electrode cell: specimen as a working electrode and a platinum counter electrode. All electrochemical experiments were performed using Autolab PGSTAT30.

The specimens were kept in a decicator for 48 hours at room temperature before surface analysis and corrosion tests. The test site was located in Ha Noi. Test specimens were exposed on a rack at 45 °C to the horizontal facing south in accordance with ISO 8565 [8]. Specimens were removed after 12; 24; 36, 48, 60 months of exposure. The sulfur dioxide (SO₂) deposition rates were determined using lead dioxide (PbO₂) and determination of chloride deposition rate was carried out by the wet candle method in accordance with ISO 9225 [9]. To determine the coating mass loss due to corrosion, the products formed during the corrosion process were removed by using the methods and the procedures described in the ISO 8407 [10]:

The weight of specimens was weighed by means of analytical balance SHIMADZU AEG-220g, with precision 10⁻⁴ gr. Corrosion rates were determined from the weight losses of specimens in accordance with ISO 9226 [12].

Average weight loss K after removal of corrosion products:

$$k = \frac{\sum_{i=1}^N \Delta m_i}{N}, g/m^2 \quad \text{with} \quad \Delta m_i = \frac{m_{0i} - m_{1i}}{S}, g/m^2$$

Where: m_{0i} (gr): the specimen weight after electroplating and conversion treatments;

m_{1i} (gr): the specimen weight after removal of corrosion product; S (m²): the specimen surface area.

Average corrosion rate II:

$$II = \frac{K \times 365}{\Delta t \times d}, \mu m/y$$

Where: K (g/m²): average weight loss; d (g/cm³): the density; Δt (days): the exposure time.

3. Results And Discussion

3.1. Surface evaluation of the passive films

The surfaces of the passive films after drying are visually inspected and the results are presented in Table 3. In general, the surfaces of all passivated samples were bright and had The iridescent colours of the passive films were clear with pink and green as the main colours for two types of the trivalent chrome conversion coatings and green and yellow for the hexavalent chrome conversion coatings.

3.2. Characteristics of climate at the test site

The samples for testing atmospheric corrosion were exposed at Ha Noi, Viet Nam. The latitude and

Table 1. Details of the conversion treatments

Coating	Treatment solution	pH	Immersion time, s	Drying temperature, °C	Specimen symbol
Zinc	-	-	-	-	Zn
Cr(VI)*	Udycro 747 (Enthone)	1.4 ÷ 1.8	30	50	747
Cr(III)**	SpectraMATE 25 (Columbia)	2.0 ÷ 2.2	60	80	SP 25
Cr(III)**	TM 3108	2.0 ÷ 2.2	60	80	TM 3108

Table 2. Chemical cleaning procedures for removal of corrosion products [11]

Specimens	Chemical	Time, s	Temperature, °C
Zn	200 g chromium trioxide (CrO ₃) Distilled water to make 1000 ml	60	80 °C
747	200 g chromium trioxide (CrO ₃) Distilled water to make 1000 ml	60	80 °C
SP 25	100 g ammonium acetate (CH ₃ COONH ₄) Distilled water to make 1000 ml	120	70 °C
TM 3108	100 g ammonium acetate (CH ₃ COONH ₄) Distilled water to make 1000 ml	120	70 °C

longitude of Ha Noi are $21^{\circ} 01' N$ and $105^{\circ} 51' E$ respectively. Ha Noi's climate is symbolic of the climate of North Vietnam. Ha Noi climate belongs to tropical monsoon temperature type: hot summer with high rainfall and cold winter, rare of rain. Located in tropical zone, Ha Noi has abundant radiation around year. Average total of radiation is accounted to 122.8 Lcal/cm^2 , sunshine hour is 1641 and annual temperature is $23.6^{\circ} C$. June is the hottest month and the temperature may reach to $38^{\circ} C$. The coldest month is recorded in January. Ha Noi receives relatively high humidity and rainfall. The average annual humidity is 79% and rainfall is 1,800mm a year. Ha Noi experiences four seasons in a year. May to September are the hot and rainy months. Dry winter lasts from November to March in next year. Autumn and Spring are transition seasons of April to October.

Environmental data were collected during the tiexposure in the test site: SO_2 and Cl^- .



Figure 1. Specimens exposure



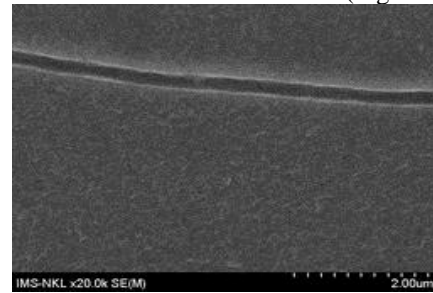
Figure 2. Measurement of pollution SO_2 , Cl^-

The sulfur dioxide (SO_2) deposition rates were determined using lead dioxide (PbO_2) and determination of chloride deposition rate was carried out by the wet candle method (Figure 3) in accordance with ISO 9225. Table 4 shows that the chloride ion concentrations is classified as S_0 and sulfur dioxide concentrations is classified as P_0 .

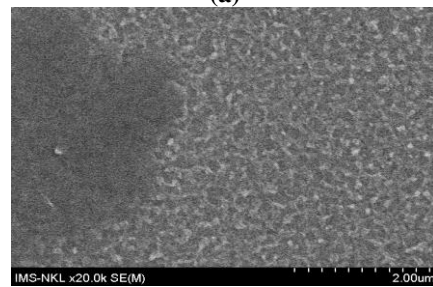
3.3. The morphology of the passive films

The surface SEM images of Zn, TM 3108, SP25 and 747

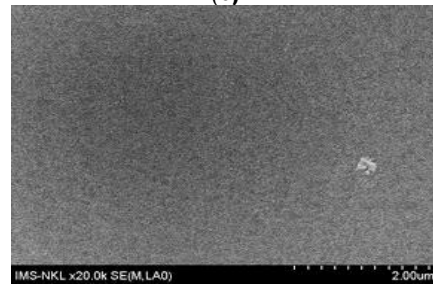
are shown in Figure 3. The surface of the Zn was porous and had homogeneous crystals with sizes ranging from 30 to 100 nm (Figure 3d). The trivalent chrome conversion coatings didn't appear cracks or cloud on the surface (Figure 3b and Figure 3c). On the hexavalent chrome conversion coatings, it could see cracks with about 200 nm width (Figure 3a).



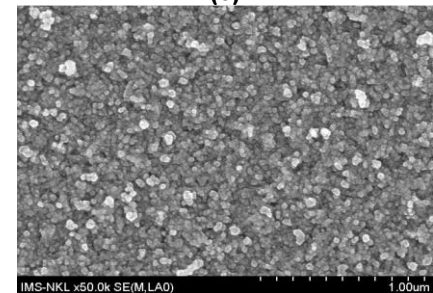
(a)



(b)



(c)



(d)

Figure 3. The surface SM images of 747 (a); SP 25 (b); TM 3108 (c) and Zn (d).

Table 3. Surface evaluation of the hexavalent and trivalent chrome conversion coatings.

Samples	Appearance of samples
747	Bright, iridescent with two main colours green and yellow
SP 25	Bright, iridescent with two main colours pink and green
TM 3108	Bright, iridescent with two main colours pink and green

Table 4. Annual average values of SO_2 and Cl^- concentrations.

Annual average	SO_2 , $mg/m^2 \cdot day$	Classification in accordance with ISO 9223	Cl^- , $mg/m^2 \cdot day$	Classification in accordance with ISO 9223 [13]
2013	$9.2 \div 9.5$	$P_0 (P \leq 10)$	$2.2 \div 2.5$	$S_0 (S \leq 3)$
2014	$9.1 \div 9.4$	$P_0 (P \leq 10)$	$2.1 \div 2.6$	$S_0 (S \leq 3)$
2015	$9.1 \div 9.3$	$P_0 (P \leq 10)$	$2.1 \div 2.4$	$S_0 (S \leq 3)$
2016	$9.3 \div 9.6$	$P_0 (P \leq 10)$	$2.3 \div 2.5$	$S_0 (S \leq 3)$
2017	$9.2 \div 9.5$	$P_0 (P \leq 10)$	$2.1 \div 2.3$	$S_0 (S \leq 3)$
2018	$9.1 \div 9.4$	$P_0 (P \leq 10)$	$2.2 \div 2.4$	$S_0 (S \leq 3)$

Results SEM image (skyward face) in Figure 4 shows that the porous corrosion products appeared on the surface of all samples after 12 months exposure. In general, corrosive products were evenly distributed on the surface of the test samples. However, the degree of corrosion varied with the type of samples. The zinc coatings are strongly corroded, creating many wide stains of corrosion. Whereas for CCCs, especially the hexavalent CCCs, the corrosion stains are smaller and less sparse. The CCCs still retain the colors of the conversion films.

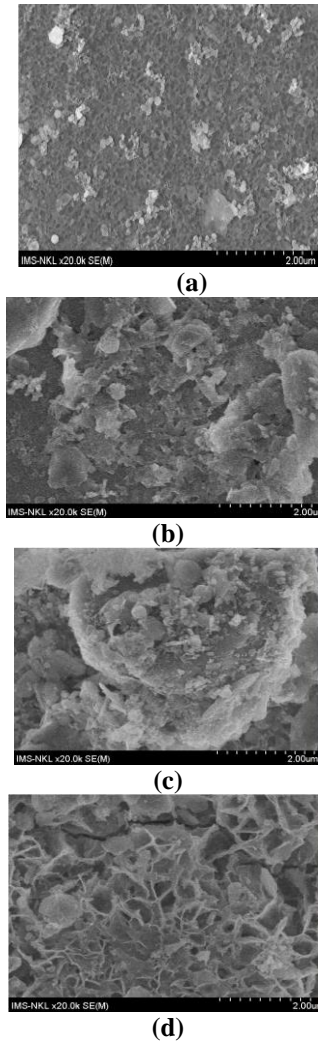


Fig. 4. SEM images of 747 (a); SP25 (b); TM 3108 (c); Zn (d) exposed for 12 months in Ha Noi, Viet Nam.

3.3. Salt spray testing

3.3.1 Salt spray testing at pH 3

Table 5. The results of the salt spray testing at pH 3.

Samples	Testing time, h		
	Initial white rust	3 – 5 % white rust	> 5 % white rust
Zn	-	0.1	0.5
747	3	5	24
SP 25	5	8	24
TM 3108	5	8	24

The salt spray testing results of the samples tested in acidic environment of pH 3 are presented in Table 5 and Figure 5. On the Zn, about 5 % of the surface area was covered with white corrosion products only in few minutes of testing and after 30 minutes, white rust covered almost the surface areas. On the SP 25 and TM 3108, white rust appeared after 5 hours of salt fog exposure. White rust appeared on the hexavalent chrome conversion coatings sooner than on the trivalent chrome conversion coatings. All samples had more than 5 % of the surface area covered with white rust after 24

hours of salt fog exposure. The trivalent chrome conversion coatings and hexavalent chrome conversion coatings were unstable in testing conditions at pH 3. Increasing time, corrosion processes occurred on the SP 25 and TM 3108 stronger than on the 747.

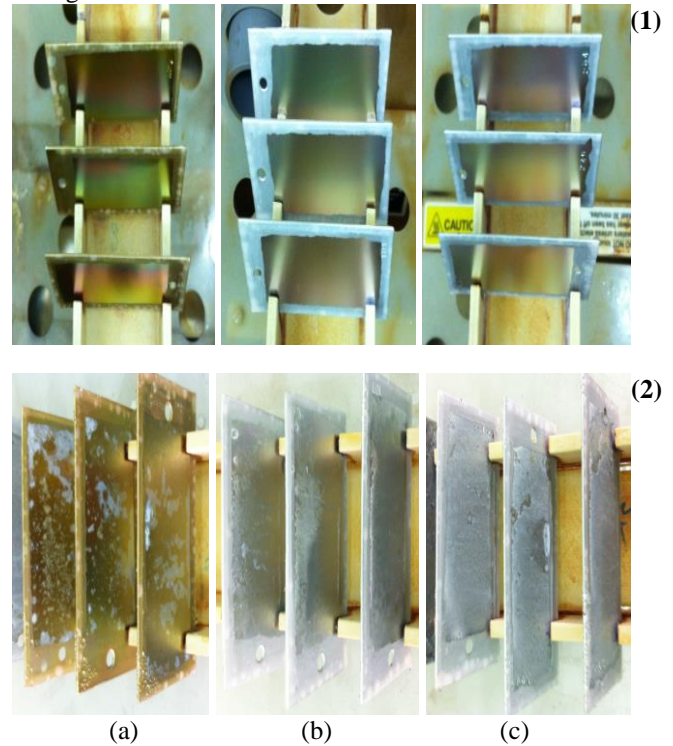


Figure 5. The images of the samples tested in salt spray at pH 3: 747 (column a), SP 25 (column b) and TM 3108 (column c) at the beginning of test (row 1), after 24 hours of salt fog exposure (row 2).

3.3.2 Salt spray testing at pH 4.5

Table 6. The results of the salt spray testing at pH 4.5

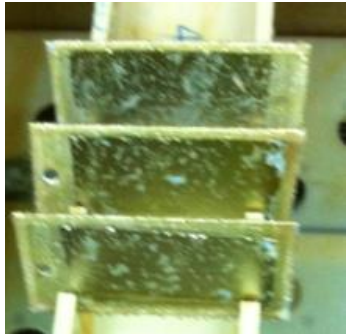
Samples	Testing time, h		
	Initial white rust	3 – 5 % white rust	> 5 % white rust
Zn	-	0.2	1
747	10	24	48
SP 25	15	22	30
TM 3108	12	20	24

The salt spray testing results of the samples tested in acidic environment of pH 4.5 are presented in Table 6 and Figure 6. On the samples with the SP 25 and TM 3108, white rust appeared correspondingly after 15 hours and 12 hours of salt fog exposure. Duration for white rust appearing on the 747 is 10 hours and after 48 hours more than 5 % of the surface area covered with rust. Despite the results were better than the ones at pH 3, the SP 25, TM 3108 and 747 were still unstable in testing conditions at pH 4.5. Increasing time, corrosion processes occurred on the SP 25, TM 3108 stronger than on the 747.

3.3.3 Salt spray testing at pH 5.5

Table 7. The results of the salt spray testing at pH 5.5.

Samples	Testing time, h		
	Initial white rust	3 – 5 % white rust	> 5 % white rust
Zn	-	0.5	1.5
747	72	120	300
SP 25	240	300	-
TM 3108	300	350	-



(a)



(b)



(c)

Figure 6. The images of the samples tested in salt spray at pH 4.5: 747 (a), SP 25 (b) and TM 3108 (c) after 48 hours of salt fog exposure.



(a)



(b)



(c)

Figure 7. The images of the samples tested in salt spray at pH 5.5: 747 (a), SP 25 (b) and TM 3108 (c) after 240 hours of salt fog exposure.

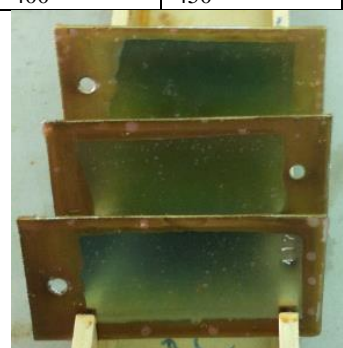
Table 7 and Figure 7 present the salt spray testing results of the samples tested in weak acidic environment of pH 5.5. TM 3108 had the highest resistance with white rust appeared after 300 hours of testing. On the samples with the SP 25, white rust appeared after 240 hours of salt fog exposure. The hexavalent chrome conversion coatings had the resistance worse than the trivalent chrome conversion coatings. Duration for white rust appearing on the 747 is 72 hours and after 300 hours more than 5 % of the surface area covered with rust. In testing conditions at pH 5.5, the corrosion resistance of the samples is as follows: TM 3108 ~ SP 25 > 747.

3.3.4 Salt spray testing at pH 6.5

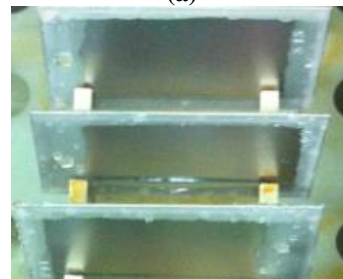
The salt spray testing results of the samples tested in neutral environment of pH 6.5 are shown in Table 8 and Figure 8. On the Zn, about 5 % of the surface area was covered with white corrosion products after 2 – 3 hours of testing and after 10 hours, white rust covered almost the surface areas. The highest resistance obtained on the TM 3108 with white rust appeared after 400 hours of salt fog exposure. In testing conditions at pH 6.5, the corrosion resistance of the samples is as follows: TM 3108 ~ SP 25 > 747.

Table 8. The results of the salt spray testing at pH 6.5.

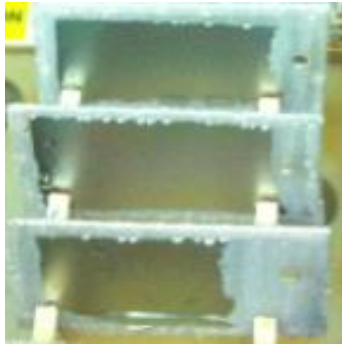
Samples	Testing time, h		
	Initial white rust	3 – 5 % white rust	> 5 % white rust
Zn	1	2	10
747	72	120	300
SP 25	250	380	-
TM 3108	400	450	-



(a)



(b)



(c)

Figure 8. The images of the samples tested in salt spray at pH 6.5: 747 (a), SP 25 (b) and TM 3108 (c) after 300 hours of salt fog exposure.

3.4. Polarization measurements

3.4.1 Polarization measurements at pH 3

Corrosion behaviour of the Zn; TM3108; SP 25 and 747 defined by potentiodynamic polarization methods in acidic environment of pH 3 are presented in Table 9 and Figure 9. Corrosion current density of the sample with the 747 was much smaller than corrosion current density of the Zn. Whereas, corrosion current density of the TM 3108 was close to corrosion current density of the Zn. The trivalent chrome conversion coatings was removed rapidly after 0.5 hours of immersing sample in 5 % NaCl solution adjusted to pH 3 with CH₃COOH. The polarization measurement results accorded with the salt spray testing results at pH 3.

Table 9. Potentiodynamic polarization data at pH 3.

Samples	E_{corr} , mV (SCE)	I_{corr} , A.cm ⁻²
Zn	-1073	1.96×10^{-5}
747	-1040	4.08×10^{-6}
SP 25	-1057	4.73×10^{-6}
TM 3108	-1058	1.12×10^{-5}

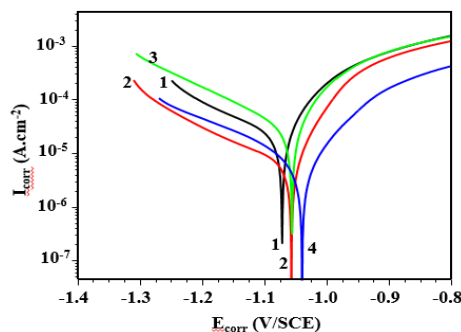


Figure 9. Polarization curves of the samples at pH 3: Zn (1), SP 25 (2), TM 3108 (3) and 747 (4).

3.4.2 Polarization measurements at pH 4.5

The potentiodynamic polarization results of the samples measured in acidic environment of pH 4.5 are presented in Table 10 and Figure 10. Corrosion current density of the sample with the 747 had the smallest value. Both of the SP25 and TM 3108 had corrosion current densities approximating to the corrosion current density of the Zn. These trivalent chrome conversion coatings were removed rapidly after 1 hours of immersing samples in 5 % NaCl solution adjusted to pH 4.5 with CH₃COOH.

Table10. Potentiodynamic polarization data at pH 4.5.

Samples	E_{corr} , mV (SCE)	I_{corr} , A.cm ⁻²
Zn	- 1103	8.37×10^{-6}
747	- 1072	1.92×10^{-6}
SP 25	- 1086	7.22×10^{-6}
TM 3108	- 1066	7.58×10^{-6}

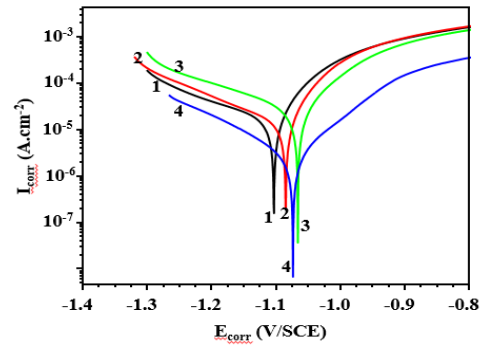


Figure 10. Polarization curves of the samples at pH 4.5: Zn (1), SP 25 (2), TM 3108 (3) and 747 (4).

3.4.3 Polarization measurements at pH 5.5

The polarization results of the samples measured in weak acidic environment of pH 5.5 are presented in Table 11 and Figure 11. All of the hexavalent chrome conversion coatings and trivalent chrome conversion coatings had corrosion current densities approximating to each other and much smaller than corrosion current density of the zinc electrodeposited sample. The polarization measurement results agreed with the salt spray testing results.

Table 11. Potentiodynamic polarization data at pH 5.5.

Samples	E_{corr} , mV (SCE)	I_{corr} , A.cm ⁻²
Zn	-1107	5.7×10^{-6}
747	-1124	5.8×10^{-7}
SP 25	-1121	2.7×10^{-7}
TM 3108	-1071	2.5×10^{-7}

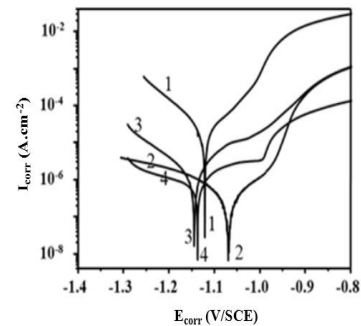


Figure 11. Polarization curves of the samples at pH 5.5: Zn (1), SP 25 (2), TM 3108 (3) and 747 (4).

3.4.4 Polarization measurements at pH 6.5

The polarization results of the samples measured in neutral environment of pH 6.5 are presented in Table 12 and Figure 12. All of the hexavalent chrome conversion coatings and trivalent chrome conversion coatings had corrosion current densities much smaller than corrosion current density of the zinc electrodeposited sample. These polarization results were also smaller than the ones of the samples measured in acidic environment of pH 5.5. The polarization measurement results agreed with the salt spray testing results.

Table 13 shows that, all of the hexavalent CCCs and trivalent CCCs before natural exposure had corrosion current densities ($1.26 \times 10^{-7} \div 1.82 \times 10^{-7}$ A/cm²) much smaller than those of the samples after 5 years natural exposure ($5.52 \times 10^{-4} \div 6.96 \times 10^{-4}$ A/cm²).

Table 12. Potentiodynamic polarization data at pH 6.5.

Samples	E_{corr} , mV (SCE)	I_{corr} , A.cm ⁻²
Zn	- 1050	7.7×10^{-6}
747	-1131	1.82×10^{-7}
SP 25	- 1110	1.26×10^{-7}
TM 3108	- 1071	1.56×10^{-7}

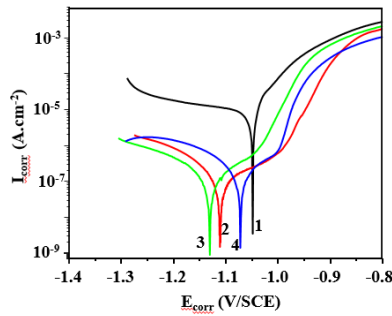


Figure 12. Polarization curves of the samples at pH 6.5: Zn (1), SP 25 (2), TM 3108 (3) and 747 (4).

Table 13. Potentiodynamic polarization data before and after 5 years natural exposure natural.

Samples	Before natural exposure		After 5 years natural exposure	
	E_{corr} , mV (SCE)	I_{corr} , A.cm ⁻²	E_{corr} , mV (SCE)	I_{corr} , A.cm ⁻²
Zn	-1050	7.7×10^{-6}	-1100	7.3×10^{-4}
747	-1131	1.82×10^{-7}	-1095	5.52×10^{-4}
SP 25	-1110	1.26×10^{-7}	-1090	6.96×10^{-4}
TM 3108	-1071	1.56×10^{-7}	-1095	5.56×10^{-4}

3.5. Corrosion rate after exposure time

Table 14 shows that, after 60 months of exposure, the loss of weight of Zn > SP25 ~ TM 3108 > 747; and the corrosion rate of Zn > SP25 ~ TM 3108 > 747. The hexavalent chrome conversion coating on zinc coating showed the best corrosion resistance.

3.6. Composition of corrosion products and surface morphology

Table 15 shows the composition of corrosion products of 747(a); Zn (b); SP25 (c); TM 3108 (d) after exposure time.

The results of analysis by means of X-ray diffraction showed that the corrosion products formed on zinc coating, trivalent CCCs, hexavalent CCCs in atmospheric conditions Ha Noi has the following distinctions specialty of the humid tropical climates. Zinc sulfate hydroxide hydrate $Zn_4SO_4(OH)_6 \cdot H_2O$; Zinc carbonate hydroxide hydrate $Zn_4CO_3(OH)_6 \cdot H_2O$; Simonkolleite $Zn_5(OH)_8Cl_2 \cdot H_2O$; Chromium sulfate $Cr_2(SO_4)_3$; Zinc chloride sulfate hydroxide hydrate $Zn_{12}(OH)_{15}(SO_4)_3Cl_3 \cdot H_2O$; Eskolaite Cr_2O_3 has been identified by means of X-ray diffraction. The variations in the relative proportions of the formed phases had a strong dependence on the changes of the content of the main pollutant such as SO_2 and chlorides as well as on the rainy and dry seasons during the annual exposure time. A thin layer of amorphous Zinc carbonate hydroxide hydrate $Zn_4CO_3(OH)_6 \cdot H_2O$ forms rapidly in humid atmosphere. The chlorides are also present in the atmosphere, so simonkolleite $Zn_5(OH)_8Cl_2 \cdot H_2O$ is locally formed. The presence of SO_2 results in the formation of Zinc sulfate hydroxide hydrate $Zn_4SO_4(OH)_6 \cdot H_2O$.

After 60 months of exposure, the hexavalent chrome conversion coating on zinc coating showed the least corrosion products.

3.7. FTIR spectra of the TM3108 and 747 after 5 years natural exposure.

Fig. 13 shows FTIR spectra acquired from 747-based coating on zinc. The band at 880 cm^{-1} is due to the vibration of Cr(VI)-O. The band at 531 cm^{-1} is due to the vibration of Cr(III)-O. The broad absorption bands at 3341 and 1638 cm^{-1} are attributable to the vibration of water or water of hydration. The band at 1127 cm^{-1} is from the vibration of SO_4^{2-} in the coating. Fig. 14 shows FTIR spectra acquired from Cr(III)-TM3108-based coating on zinc electroplating after 5 years natural exposure in Ha Noi. The broad absorption bands at

Table 14. Results loss of weight and corrosion rate after exposure time.

Specimen	Zn	TM3108	SP25	747	Zn	TM3108	SP25	747
	Loss of weight, g/m ²				Corrosion rate, $\mu\text{m}/\text{year}$			
12 months	5.5	2.0	2.2	0.5	$0.7 \div 0.8$	$0.2 \div 0.3$	$0.2 \div 0.4$	$0.06 \div 0.1$
24 months	15	9.6	9.8	6.8	$1.0 \div 1.1$	$0.6 \div 0.7$	$0.6 \div 0.7$	$0.4 \div 0.5$
36 months	28	14	14.5	9.8	$1.3 \div 1.4$	$0.6 \div 0.7$	$0.6 \div 0.7$	$0.4 \div 0.5$
48 months	41	18	18.9	14.1	$1.4 \div 1.5$	$0.6 \div 0.7$	$0.6 \div 0.7$	$0.4 \div 0.5$
60 months	55	23	23.8	19.7	$1.5 \div 1.6$	$0.6 \div 0.7$	$0.6 \div 0.7$	$0.5 \div 0.6$

Table 15. The corrosion products formed on zinc coating, trivalent CCCs, hexavalent CCCs (x: the presence of corrosion products).

Corrosion products	Exposure time, month	Specimen			
		Zn	TM3108	SP25	Cr ⁶⁺
Zinc sulfate hydroxide hydrate $Zn_4SO_4(OH)_6 \cdot H_2O$	12	x	x	x	
	24	x	x	x	x
	48	x	x	x	x
	60	x	x	x	x
Zinc carbonate hydroxide hydrate $Zn_4CO_3(OH)_6 \cdot H_2O$	24	x			x
	48	x	x	x	
	60	x		x	
Simonkolleite $Zn_5(OH)_8Cl_2 \cdot H_2O$	12	x			
	24	x	x	x	
	48			x	
	60			x	
Chromium Sulfate $Cr_2(SO_4)_3$	24		x		x
Zinc chloride sulfate hydroxide hydrate $Zn_{12}(OH)_{15}(SO_4)_3Cl_3 \cdot H_2O$	24		x		
	60		x		
Eskolaite Cr_2O_3	48				x
	60		x		x

3440 and 1625 cm^{-1} are attributable to the vibration of water or water of hydration. The band at 1126 cm^{-1} is from the vibration of SO_4^{2-} in the coating. The band at 538 cm^{-1} is due to the vibration of Cr(III)-O. No band at 880 cm^{-1} has been observed, which means that no Cr(VI) exists in trivalent CCCs on zinc electroplating.

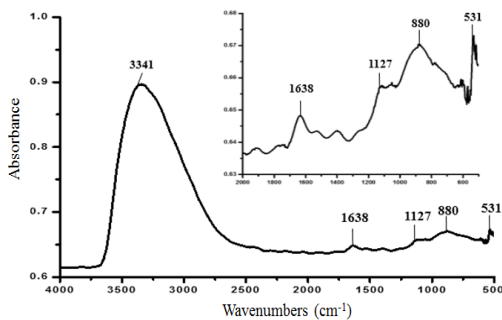


Fig 13. FTIR spectra acquired from 747 after 5 years natural exposure in Ha Noi.

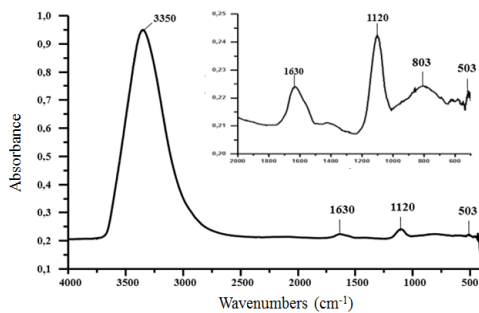


Fig 14. FTIR spectra acquired from TM3108 after 5 years natural exposure in Ha Noi.

4. Conclusions

1. The hexavalent chrome conversion coatings and trivalent chrome conversion coatings were unstable in testing conditions at pH 3 and pH 4.5. In testing conditions at pH 5.5, the corrosion resistance of the samples is as follows: TM 3108 is close to SP 25 and both are greater than 747. At pH 6.5, the corrosion resistance of the trivalent chrome conversion coatings TM 3108 was the best. The polarization measurement results accorded with the salt spray testing results.

2. After 60 months of exposure, the loss of weight of samples decreases in order $\text{Zn} > \text{SP25} \sim \text{TM 3108} > 747$; and the corrosion rate of samples also decreases in order $\text{Zn} > \text{SP25} \sim \text{TM 3108} > 747$. The corrosion resistance of samples decreases in order $747 > \text{SP25} \sim \text{TM 3108} > \text{Zn}$. The hexavalent CCCs on zinc coating showed the best corrosion resistance and the least corrosion products. All of the hexavalent CCCs and trivalent CCCs before natural exposure had corrosion current densities much smaller than those of the

samples after 5 years natural exposure. No Cr(VI) exists in trivalent CCCs on zinc electroplating after 5 years natural exposure.

References

1. X. Zhang, W.G. Sloof, A. Hovestadb, E.P.M. van Westing, H. Terry, J.H.W. de Wit, Characterization of chromate conversion coatings on zinc using XPS and SKPFM, *Surface & Coatings Technology*, 197 (2005) 168–176.
2. Yu-Tsern Chang, Niann-Tsyw Wen, We-Kun Chen, Ming-Der Ger, Guan-Tin Pan, Thomas C.-K. Yang, The effects of immersion time on morphology and electrochemical properties of the Cr(III)-based conversion coatings on zinc coated steel surface, *Corrosion Science*, 50 (2008) 3494–3499.
3. Niann-Tsyw Wen, Chao-Sung Lin, Ching-Yuan Bai, Ming-Der Ger, Structures and characteristics of Cr(III)-based conversion coatings on electrogalvanized steels, *Surface & Coatings Technology*, 203 (2008) 317–323.
4. C. R. Tomachuk, C. I. Elsner, A. R. Di Sarli, O. B. Ferraz, Morphology and corrosion resistance of Cr(III)-based conversion treatments for electrogalvanized steel, *J. Coat. Technol. Res* 7 (2010) 493–502.
5. J. García-Antón, R.M.Fernández-Domene, R.Sánchez-Tovar, C.Escrivà-Cerdán, R. Leiva-García, V.García, A.Urtiaga, Improvement of the electrochemical behaviour of Zn-electroplated steel using regenerated Cr (III) passivation baths, *Chemical Engineering Science* 111 (2014) 402 – 409.
6. A.R. Di Sarli, J.D. Culcasi, C.R. Tomachuk, C.I. Elsner, J.M. Ferreira-Jr, I. Costa, A conversion layer based on trivalent chromium and cobalt for the corrosion protection of electrogalvanized steel, *Surface & Coatings Technology* 258 (2014) 426–436.
7. Technical Manual ENTHONE OMI Inc.
8. ISO 8565-92: Metal and Alloys – Atmospheric Corrosion Test – General requirement for Field Test.
9. ISO 9225: Corrosion of metals and alloys – Corrosivity of atmospheres – Measurement of pollution.
10. ISO 8407 – 91: Corrosion of metals and alloys – Removal of corrosion products from corrosion test specimens.
11. Nguyen Thi Thanh Huong, Le Ba Thang, The selection liquid removing of corrosion product for zinc coating and trivalent chrome conversion coating, hexavalent chrome conversion coating on zinc electroplating, *Vietnam Journal of Chemistry T.52(6B)* (2014) 149 – 152.
12. ISO 9226: Corrosion of metals and alloys - corrosivity of Atmospheres - Method of determination of corrosivity using the corrosion loss standard specimens.
13. ISO 9223: Corrosion of metal and alloys – Corrosivity of atmosphere – Classification.